Phosphate-binding tag: A new tool to visualize phosphorylated proteins

Eiji Kinoshita[1,2]*, Emiko Kinoshita-Kikuta[1], Kei Takiyama[1], Tohru Koike[1,2]*

[1]Department of Functional Molecular Science, Graduate School of Biomedical Sciences, Hiroshima University, Kasumi 1-2-3, Hiroshima 734-8551, Japan.
[2]Frontier Center for Microbiology, Hiroshima University, Kasumi 1-2-3, Hiroshima 734-8551, Japan.

* To whom correspondence should be addressed: Department of Functional Molecular Science, Graduate School of Biomedical Sciences, Hiroshima University, Kasumi 1-2-3, Hiroshima 734-8551, Japan.
Tel: +81-82-257-5281; Fax: +81-82-257-5336
E-mail: tkoike@hiroshima-u.ac.jp, kinoeiji@hiroshima-u.ac.jp

Running Title: Visualization of phosphorylated proteins

The abbreviations used are: AP, alkaline phosphatase; EGF, epidermal growth factor; HRP–SA, horseradish peroxidase-conjugated streptavidin; *Phos-tag*, phosphate-binding tag; TC-PTP, T-cell protein tyrosine phosphatase

SUMMARY

We introduce two methods for the visualization of phosphorylated proteins using alkoxide-bridged dinuclear metal (*i.e.*, Zn^{2+} or Mn^{2+}) complexes as novel phosphate-binding tag (*Phos-tag*) molecules. Both Zn^{2+}– and Mn^{2+}–*Phos-tag* molecules preferentially capture phosphomonoester dianions bound to Ser, Thr, and Tyr residues. One method is based on an enhanced chemiluminescence (ECL) system using biotin-pendant Zn^{2+}–*Phos-tag* and horseradish peroxidase-conjugated streptavidin (HRP–SA). We demonstrate the electroblotting analyses of protein phosphorylation status by the phosphate-selective ECL signals. Another method is based on the mobility shift of phosphorylated proteins in SDS-PAGE with polyacrylamide-bound Mn^{2+}–*Phos-tag*. Phosphorylated proteins in the gel are visualized as slower migration bands compared with corresponding dephosphorylated proteins. We demonstrate the kinase and phosphatase assays by the phosphate-affinity electrophoresis (Mn^{2+}–*Phos-tag* SDS-PAGE).

Keywords: Phosphoproteomics; Electroblotting analysis; Chemiluminescence detection; Phosphate-affinity electrophoresis; Phosphorylated protein; Phosphorylation

INTRODUCTION

Phosphorylation is a fundamental covalent post-translational modification that regulates the function, localization, and binding specificity of target proteins (1, 2). Organisms utilize this reversible reaction of proteins to control many cellular activities, including signal transduction, apoptosis, gene expression, cell cycle progression, cytoskeletal regulation, and energy metabolism. Abnormal protein phosphorylations are deeply related to carcinogenesis and neuropathogenesis. Methods for determining the phosphorylation status of proteins are thus very important with respect to the evaluation of diverse biological and pathological processes.

Recently, we have reported that a dinuclear metal complex (*i.e.*, 1,3-bis[bis(pyridin-2-ylmethyl)amino]propan-2-olato dizinc(II) complex) acts as a novel phosphate-binding tag, *Phos-tag* (3) in an aqueous solution at a neutral pH (*e.g.*, K_d = 25 nM for phenyl phosphate dianion) (4). The *Phos-tag* (see Fig. 1) has a vacancy on two metal ions that is suitable for the access of a phosphomonoester dianion as a bridging ligand. The resulting 1:1 phosphate-binding complex, $ROPO_3^{2-}$–(Zn^{2+}–*Phos-tag*)$^{3+}$, has a total charge of +1. The anion selectivity indexes of the phenyl phosphate dianion against SO_4^{2-}, CH_3COO^-, Cl^-, and the bisphenyl phosphate monoanion at 25 ˚C are 5.2×10^3, 1.6×10^4, 8.0×10^5, and $>2 \times 10^6$, respectively. These findings have contributed to the development of procedures for matrix-assisted laser desorption/ionization time-of-flight mass spectrometry (MALDI-TOF-MS) for the analysis of phosphorylated compounds (*e.g.*, phosphopeptides and phospholipids) (5–7), immobilized metal affinity chromatography (IMAC) for the separation of phosphopeptides and phosphorylated proteins (8), and surface plasmon resonance (SPR) analysis for reversible peptide phosphorylation (9). In this study, we demonstrated two novel applications of the *Phos-tag* molecules: one is the chemiluminescence detection of whole phosphorylated proteins on electroblotting membranes using biotinylated Zn^{2+}–*Phos-tag* and HRP–SA. Another is a simple SDS-PAGE for the separation of

a phosphorylated protein and the corresponding nonphosphorylated one, where polyacrylamide-bound Mn^{2+}–*Phos-tag* was used as a phosphate-binding moiety.

EXPERIMENTAL PROCEDURES

Materials. Acrylic acid, boric acid, bovine intestinal mucosa alkaline phosphatase (AP), bovine milk α-casein, bovine milk β-casein, carbonic anhydrase, chicken egg ovalbumin, human serum albumin, NaCl, *O*-phosphoryl serine, *O*-phosphoryl tyrosine, and porcine pepsin were purchased from Sigma-Aldrich (St. Luis, MO, USA). 1-Ethyl-3-(3-dimethylaminopropyl)-carbodiimide hydrochloride and 4-methoxyphenol were purchased from Tokyo Kasei Kogyo (Tokyo, Japan). A Good's buffer, HEPES (2-[4-(2-hydroxyethyl)-1-piperazinyl]ethanesulfonic acid) was purchased from Dojindo (Kumamoto, Japan). Thin-layer and silica gel column chromatographies were performed using a Merck Silica gel TLC plate No. 05554, silica gel 60 F_{254} (Darmstadt, Germany) and Fuji Silysia Chemical NH-DM 1020 silica gel (Kasugai, Japan), respectively. Harmane (1-methyl-9*H*-pyrido[3,4-*b*]indole) and 2'4'6'-trihydroxyacetophenone were purchased from Aldrich Chemical Company (Milwaukee, WI, USA). Bovine serum albumin was purchased from New England Biolabs (Beverly, MA, USA). β-Galactosidase was purchased from Toyobo (Osaka, Japan). Ampholine (pH 3.5 – 10.0) for IEF, broad-range protein molecular weight standards, ECL-plus- western blotting detection reagent, HRP-conjugated anti-mouse IgG antibody, HRP-conjugated anti-pTyr monoclonal antibody (clone PY20), HRP-conjugated anti-rabbit IgG antibody, HRP-conjugated streptavidin, and PVDF membrane (Hybond P) were purchased from GE Healthcare/Amersham Bioscience (Piscataway, NJ, USA). Protein kinase A, recombinant human histone H1.2, and recombinant human T-cell protein tyrosine phosphatase (TC-PTP) were purchased from Calbiochem (La Jolla, CA, USA). A431 cell lysate, EGF-stimulated A431 cell lysate, alkaline phosphatase treated EGF-stimulated A431 cell lysate were purchased from Santa Cruz Biotechnology (Santa Cruz, CA, USA). Rabbit anti-pSer polyclonal antibody was purchased from Zymed Laboratories (South San Francisco, CA, USA). Microcon YM30 and YM3 filter units were purchased from Millipore (Bedford, MA, USA). Pro-Q Diamond phosphoprotein gel stain and

SYPRO Ruby protein gel stain were purchased from Invitrogen (Carlsbad, CA, USA). Acrylamide, 6-aminohexanoic acid, ammonium persulfate, CH_3COONa, Coomassie Brilliant Blue R-250 (CBB), glycerol, glycine, 2-mercaptoethanol, *N,N'*-methylenebisacrylamide, nonidet P-40, disodium phenyl phosphate, SDS, TEMED, Tween 20, and tris(hydroxymethyl)aminomethane (Tris) were purchased from Nacalai Tesque (Kyoto, Japan). Anti-pMAP kinase 1/2 (Erk1/2) (clone 12D4), MAP kinase assay kit (containing myelin basic protein (MBP) and anti-pMBP monoclonal antibody), MEK1 assay kit (containing recombinant MEK1 and recombinant unactive MAP kinase 2/Erk2), recombinant Abl, recombinant Abltide-GST, and recombinant MAP kinase 2/Erk2 were purchased from Upstate (Lake Placid, NY, USA). 3MM paper was purchased from Whatman Japan (Tokyo, Japan). Acetone, $CHCl_3$, CH_2Cl_2, CH_3CN, CH_3COOH, HCl, H_3PO_4, MeOH, $MnCl_2$, NaOH, and $Zn(NO_3)_2 \cdot 6H_2O$ were purchased from Yoneyama Yakuhin Kogyou (Osaka, Japana). Bromophenol blue, NaH_2PO_4, NH_3, and urea were purchased from Katayama Chemical (Osaka, Japana). All reagents and solvents used were purchased at the highest commercial quality and used without further purification. All aqueous solutions were prepared using deionized and distilled water.

Apparatus. IR spectrum was recorded on a Horiba FT-710 infrared spectrometer with a KCl pellet (Real Crystal IR Card) at 20 ± 2 ˚C. ^1H (500 MHz) and ^{13}C (125 MHz) NMR spectra at 25.0 ± 0.1 ˚C were recorded on a JEOL LA500 spectrometer. Tetramethylsilane (in $CDCl_3$) (Merck) was used as an internal reference for ^1H and ^{13}C NMR measurements. MALDI-TOF MS spectra (positive reflector mode) were obtained on a Voyager RP-3 BioSpectrometry Workstation (PerSeptive Biosystems) equipped with a nitrogen laser (337 nm, 3-ns pulse). Time-to-mass conversion was achieved by external calibrations using peaks for a-cyano-4-hydroxycinnamic acid (*m/z* 190.05 for $M + H^+$) and a peptide, Ac-Ile-Tyr-Gly-Glu-Phe-NH_2 (*m/z* 691.31 for $M + Na^+$). The pH measurement was conducted with a Horiba F-12 pH meter (Kyoto, Japan) and a combination pH

electrode Horiba-6378, which was calibrated using pH standard buffers (pH 4.01 and 6.86) at 25 ˚C. Fluorescence gel images were acquired on a FLA 5000 laser scanner (Fujifilm, Tokyo, Japan). Pro-Q Diamond dye (10) was detected by 532-nm excitation with a 575-nm bandpass emission filter. SYPRO Ruby dye (11) was detected by 473-nm excitation with a 575-nm bandpass emission filter. A LAS 3000 image analyzer (Fujifilm) was used for the observation of chemiluminescence.

Synthesis of acrylamide-pendant *Phos-tag* ligand. Amino-pendant *Phos-tag* ligand (*N*-(5-(2-aminoethylcarbamoyl)pyridin-2-ylmetyl)-*N,N',N'*-tris(pyridin-2-yl-methyl)-1,3-diaminopropan-2-ol) was synthesized as described previously (8). A CH_2Cl_2 solution (5 mL) of 1-ethyl-3-(3-dimethylaminopropyl)-carbodiimide hydrochloride (92 mg, 0.48 mmol) was added dropwise to a solution of *N*-(5-(2-aminoethylcarbamoyl)pyridin-2-ylmetyl)-*N,N',N'*-tris(pyridin-2-yl-methyl)-1,3-diaminopropan-2-ol (0.21 g, 0.40 mmol), acrylic acid (35 mg, 0.48 mmol), and 4-methoxyphenol (0.30 mg) in 15 mL CH_2Cl_2 at 0 ˚C for 5 min. The reaction mixture was stirred for 3 h at room temperature under a nitrogen atmosphere. After the solvent had been evaporated, the residue was dissolved in 100 mL $CHCl_3$. The $CHCl_3$ solution was washed with 0.5 M HEPES-NaOH buffer (pH 7.8, 50 mL ×5) and evaporated. The residue was purified by silica gel column chromatography (eluent; CH_2Cl_2/MeOH = 50:0 to 50:1) to obtain acrylamido-pendant *Phos-tag* ligand (*N*-(5-(2-acryloylaminoethylcarbamoyl)pyridin-2-ylmetyl)-*N,N',N'*-tris(pyridin-2-yl-methyl)-1,3-diaminopropan-2-ol) as a pale yellow oil (124 mg, 0.21 mmol, 53% yield) : TLC (eluent; CH_3CN/MeOH/28% aquous NH_3 = 4:1:1) R_f = 0.70. IR (cm^{-1}): 3263, 3061, 2928, 2828, 1652, 1594, 1569, 1539, 1478, 1436, 1408, 1365, 1316, 1248, 1150, 1122, 1094, 1048, 983, 806, 763, 733. ^{1}H NMR ($CDCl_3$): δ 2.56–2.69 (4H, m, NCCCHN), 3.57–3.66 (4H, m, CONCCH and CONCHC), 3.80–3.94 (9H, m, NCCHCN and PyCHN), 5.65 (1H, d, *J* = 10.3 Hz, COC=CH), 6.11 (1H, dd, *J* = 17.0 and 10.3 Hz, COCH=C), 6.29 (1H, d, *J* = 17.0 Hz, COC=CH), 6.60 (1H, bs, NHCOC=C), 7.13 (3H, t, *J* = 6.2 Hz, PyH), 7.34 (3H, d, *J* = 7.8 Hz, PyH), 7.44 (2H,

d, J = 8.0 Hz, PyH), 7.59 (3H, td, J = 7.7 and 1.8 Hz, PyH), 7.73 (1H, bs, PyCONH), 7.99 (1H, dd, J = 8.0 and 2.3 Hz, PyH), 8.50 (3H, d, J = 4.3 Hz, PyH), 8.90 (1H, d, J = 1.8 Hz, PyH). ^{13}C NMR ($CDCl_3$): δ 39.7, 41.0, 58.9, 60.5, 60.8, 67.2, 122.0, 122.6, 123.0, 126.7, 128.0, 130.5, 135.4, 136.4, 147.7, 148.78, 148.83, 159.0, 159.2, 162.6, 166.4, 167.1. MALDI-TOF MS: metal-free ligand (HL) in a 50% (v/v) CH_3CN solution containing 2′,4′,6′-trihydroxyacetophenone (5 mg/mL); *m/z* 595.3 for M + H^+, 1:1 phosphate-bound dizinc(II) complex (Zn_2L^{3+}–$HOPO_3^{2-}$) in a 50% (v/v) CH_3CN solution containing 2'4'6'-trihydroxyacetophenone (5 mg/mL), 1.0 mM $Zn(CH_3COO)_2$, 0.50 mM HL, and 5.0 mM NaH_2PO_4-NaOH (pH 6.9); *m/z* 817.1, 1:1 phenyl phosphate-bound dimanganese(II) complex (Mn_2L^{3+}–*Ph*OPO_3^{2-}) in a 50% (v/v) acetone solution containing Harmane (5 mg/mL), 0.40 mM $MnCl_2$, 0.20 mM HL, 0.20 mM disodium phenyl phosphate, and 10 mM boric acid-NaOH (pH 9.0); *m/z* 875.2.

Preparation of a complex of biotin-pendant Zn^{2+}–*Phos-tag* and HRP-conjugated streptavidin. A MeOH solution of a biotin-pendant *Phos-tag* ligand (0.10 M) was diluted with an aqueous solution containing 10 mM Tris-HCl (pH 7.5), 0.10 M NaCl, and 0.1% (v/v) Tween 20 (TBS-T solution) by a factor of 10. The obtained solution of the 10 mM biotin-pendant *Phos-tag* ligand (solution-L) was stored at room temperature. To prepare the 4:1 complex of biotin-pendant Zn^{2+}–*Phos-tag* and HRP–SA, solution-L (10 μL), an aqueous solution of 10 mM $Zn(NO_3)_2$ (20 μL), a commercially available solution of HRP–SA (1 μL), and TBS-T (469 μL) were mixed and allowed to stand for 30 min at room temperature. The mixed solution was put into a Microcon YM 30 filter unit and centrifuged for 10 min at 14,000 ×*g* to remove excess biotin-pendant Zn^{2+}–*Phos-tag*. The remaining solution (< 10 μL) in the reservoir was diluted with 30 mL of a TBS-T solution and stored at 4˚C (Zn^{2+}–*Phos-tag*-bound HRP–SA solution).

SDS-PAGE. Polyacrylamide gel electrophoresis was conducted according to

Laemmli's method (12). Normal SDS-PAGE was usually performed at 35 mA/gel at room temperature in a 1-mm-thick, 9-cm-wide, and 9-cm-long gel on a PAGE apparatus (model AE6500; Atto, Tokyo, Japan). The gel consisted of 1.8 mL of a stacking gel (4.0% (w/v) polyacrylamide, 125 mM Tris-HCl (pH 6.8), and 0.1% (w/v) SDS) and 6.3 mL of a separating gel (7.5 – 12.5% (w/v) polyacrylamide, 375 mM Tris-HCl (pH 8.8), and 0.10% (w/v) SDS). For Mn^{2+}–*Phos-tag* SDS-PAGE, acrylamide-pendant *Phos-tag* ligand (50 – 150 μM) and 2 equivalent $MnCl_2$ were added to the separating gel before polymeization. An acrylamide stock solution was prepared as a mixture of a 29:1 ratio of acrylamide to *N,N'*-methylenebisacrylamide. The electrophoresis running buffer (pH 8.4) was 25 mM Tris and 192 mM glycine containing 0.1% (w/v) SDS. Sample proteins were resolved in an SDS-PAGE loading buffer (65 mM Tris-HCl (pH 6.8), 3.0% (w/v) SDS, 15% (v/v) 2-mercaptoethanol, 30% (v/v) glycerol, and 0.1% (w/v) bromophenol blue). The sample solutions were heated for 5 min at 95 ˚C before gel loading.

Pro-Q Diamond, SYPRO Ruby, and CBB gel staining. After electrophoresis, gels were fixed in an aqueous solution containing 40% (v/v) MeOH and 10% (v/v) CH_3COOH for 30 min. To stain phosphorylated proteins with Pro-Q Diamond (10), the fixed gels were washed in water for 30 min, incubated with Pro-Q Diamond phosphoprotein gel stain for 3 h, and then washed in 50 mM CH_3COONa-CH_3COOH (pH 4.0) buffer containing 20% (v/v) CH_3CN for 3 – 12 h. For CBB staining, fixed gels were incubated with a CBB solution (0.1% (w/v) CBB, 10% (v/v) CH_3COOH, and 40% (v/v) MeOH) for 1 h, and then washed in an aqueous solution containing 25% (v/v) MeOH and 10% (v/v) CH_3COOH until the background was clear. For SYPRO Ruby staining (11), fixed gels or Pro-Q Diamond-stained gels were incubated with SYPRO Ruby protein gel stain for 2 h, and then washed in 25% (v/v) MeOH and 10% (v/v) CH_3COOH for 2 h.

Two-dimensional polyacrylamide gel electrophoresis. A431 cell lysate solved

in a RIPA buffer was desalted using Microcon YM3 filter units, and resolved in a sample buffer for IEF (9.5 M urea, 2% (w/v) nonidet P-40, 2% (w/v) ampholine, and 5% (v/v) 2-mercaptoethanol) to become 2.5 μg of protein/μL. An IEF disc gel (2-mm-diameter and 12-cm-long) was consisted of 9.2 M urea, 4% (w/v) acrylamide, 0.2% (w/v) *N,N'*-methylenebisacrylamide, 0.1% (v/v) TEMED, 1.5% (w/v) nonidet P-40, 2% (w/v) ampholine, and 0.015% (w/v) ammonium persulfate. IEF was performed using Atto SJ-1060DCII. The electrode buffer of positive pole (11 mM H_3PO_4, 0.75 L) was poured into lower chamber, and the disc gels were set. Sample solutions (50 μg of protein/20 μL) were applied, and 20μL of a sample protection buffer (4.5 M urea and 1% (w/v) ampholine) was put on the sample layer, and electrode buffer of negative pole (25 mM NaOH, 450 mL) was poured into upper chamber. IEF was carried out at 400 V for 16 h at room temperature without cooling. After IEF electrophoresis, a disc gel was soaked twice for 15 min with a 0.25 M Tris-HCl (pH 6.8) buffer containing 2.5% (w/v) SDS, 5% (v/v) 2-mercaptoethanol, and 10% (w/v) glycerol. And then, SDS-PAGE (12.5 % (w/v) polyacrylamide) was performed at 50 mA/gel at room temperature using 1-mm-thick, 13.5-cm-wide, and 13.5-cm-long gel (model AE-6200, Atto).

Electroblotting. The separated proteins in a polyacrylamide gel were electroblotted to PVDF membranes for 2 h using a semi-dry blotting system (Nippon Eido NB-1600, Tokyo, Japan) at 2 mA/cm^2 with three kinds of blotting solutions (solutions A, B, and C). After normal SDS-PAGE, the gel was soaked in solution B (25 mM Tris and 5% (v/v) MeOH) for 10 min. After Mn^{2+}–*Phos-tag* SDS-PAGE, the gel was soaked in solution B containing 1.0 mM EDTA for 10 min and then soaked in solution B for 10 min. Three 3MM papers were soaked in solution A (25 mM Tris, 40 mM 6-aminohexanoic acid, and 5% (v/v) MeOH) and piled on the negative pole board. The gel, the PVDF membrane, and a piece of 3MM paper were soaked in solution B and piled up in order. Then, two pieces of 3MM paper soaked in solution C (0.30 M Tris and 5% (v/v) MeOH) were piled up.

Finally, they were covered with the positive pole board, and electricity was supplied.

Probing with Zn^{2+}–*Phos-tag*-bound HRP-SA. A protein-blotted PVDF membrane was soaked in a TBS-T solution at least for 1 h. The membrane was incubated with the Zn^{2+}–*Phos-tag*-bound HRP–SA solution (1 mL/5 cm^2) in a plastic bag for 30 min and washed twice with a TBS-T solution (10 mL/5 cm^2) for 5 min each time at room temperature. The chemiluminescence was observed using an appropriate volume of ECL-plus solution.

Probing with antibody. A blotting membrane was blocked by 1% (w/v) bovine serum albumin in TBS-T solution for 1 h. For detection of phosphorylated proteins on tyrosine residue, the membrane was probed with HRP-conjugated anti-pTyr monoclonal antibody (clone PY20) (0.5 μg/mL in TBS-T, 1 mL/5 cm^2) in a plastic bag for 1 h, and washed twice with TBS-T solution (10 mL/5 cm^2) each for 10 min, and then the chemiluminescence was observed. For detection of phosphorylated proteins on serine residue, the membrane was probed with rabbit anti-pSer polyclonal antibody (1 μg/mL in TBS-T, 1 mL/5 cm^2) in a plastic bag for 1 h, washed twice with TBS-T solution (10 mL/5 cm^2) each for 10 min, probed with HRP-conjugated anti-rabbit IgG antibody (0.1 μg/mL in TBS-T, 1 mL/5 cm^2) in a plastic bag for 1 h, and washed twice with TBS-T solution (10 mL/5 cm^2) each for 10 min, and then the chemiluminescence was observed. For detection of phosphorylated MBP on threonine residue, the membrane was probed with anti-pMBP monoclonal antibody (clone P12) (0.5 μg/mL in TBS-T solution, 1 mL/5 cm^2) in a plastic bag for 1 h, washed twice with TBS-T solution (10 mL/5 cm^2) each for 10 min, probed with HRP-conjugated anti-mouse IgG antibody (0.1 μg/mL in TBS-T, 1 mL/5 cm^2) in a plastic bag for 1 h, and washed twice with TBS-T solution (10 mL/5 cm^2) each for 10 min, and then the chemiluminescence was observed. For phosphorylated MAP kinase 1/2 (Erk1/2) detection, the membrane was probed

with anti-phospho MAP kinase 1/2 antibody (clone 12D4) (0.1 μg/mL in TBS-T solution, 1 mL/5 cm^2) in a plastic bag for 1 h, washed twice with TBS-T solution (10 mL/5 cm^2) each for 10 min, probed with HRP-conjugated anti-mouse IgG antibody (0.1 μg/mL in TBS-T, 1 mL/5 cm^2) in a plastic bag for 1 h, and washed twice with TBS-T solution (10 mL/5 cm^2) each for 10 min, and then the chemiluminescence was observed.

Reprobing of the blotting membranes. For elimination of biotin-pendant Zn^{2+}–*Phos-tag* and HRP–SA or antibodies from the blotting membrane after ECL analysis, the membranes were incubated with a stripping buffer (25 mL/5 cm^2) consisting of 62.5 mM Tirs-HCl (pH 6.8), 2% (w/v) SDS, and 0.10 M 2-mercaptoethanol for 20 min at 50 ˚C, washed 3 times with TBS-T solution (25 mL/5 cm^2) each for 1 h at room temperature, and remaining proteins on the membrane were probed with the other antibody.

Kinase assays. Phosphorylations of Abltide-GST catalyzed with Abl, MBP catalyzed with MAP kinase, and unactive MAP kinase 2/Erk2 catalyzed with MEK1 were performed using assay dilution buffer I (ADBI), magnesium/ATP cocktail substrate solutions and enzyme solutions obtained from Upstate without any dilutions. The component of each solution was as follows: ADBI consists of 20 mM MOPS (pH 7.2), 25 mM β-glycerol phosphate, 5.0 mM EGTA, 1.0 mM sodium orthovanadate, and 1.0 mM dithiothreitol. Magnesium/ATP cocktail consists of 75 mM $MgCl_2$ and 0.50 mM ATP in ADBI. Recombinant abltide-GST (0.5 mg) was dissolved in 0.50 mL of 50 mM Tris-HCl (pH 8.0), 0.15 M NaCl, 20 mM glutathione, and 20 % glycerol. MBP (2 mg) were dissolved in 1.0 mL of ADBI. Recombinant unactive MAP kinase 2/Erk2 (50 μg) was dissolved in 0.20 mL of 50 mM Tris-HCl (pH 7.5), 0.15 M NaCl. 0.10 mM EGTA, 0.03% Briji-35, 0.1% 2-merxaptoethanol, 1 mM benzamidine, 0.10 mM PMSF, and 50% glycerol. Recombinant Abl (5 μg) was dissolved in 50 μL of 50 mM Tris-HCl (pH 7.5), 0.27 M sucrose, 0.15 M NaCl, 1.0

mM benzamidine, 0.20 mM PMSF, 0.10 mM EGTA, 0.1% 2-mercaptoethanol, and 0.03% Briji 35. Recombinant MAP kinase 2/Erk2 (5 μg) was dissolved in 50 μL of 50 mM Tris-HCl (pH 7.5), 0.15 M NaCl, 0.10 mM EGTA, 0.03% Brij 35, 50 % glycerol, 1.0 mM benzamidine, 0.20 mM PMSF, and 0.1% 2-mercaptoethanol. Recombinant MEK1 (5 μg) was dissolved in 50 μL of 50 mM Tris-HCl (pH 7.5), 0.10 mM EGTA, 0.15 M NaCl, 0.1% 2-mercaptoethanol, 0.03% Brij 35, 1.0 mM benzamidine, 0.20 mM PMSF, and 5% glycerol. Time-dependent phosphorylations of substrates were performed as follows. In case of phosophorylation of Abltide-GST, 0.14 mL of ADBI, 39 μL of magnesium/ATP cocktail, 20 μL of Abltide-GST (20 μg), and 1.0 μL of recombinant Abl (0.1 μg) were incubated at 30 ˚C. In case of MBP, 29 μL of ADBI, 10 μL of magnesium/ATP cocktail, 10 μL of MBP (20 μg), and 1.0 μL of recombinant MAP kinase 2/Erk2 (0.1 μg) were incubated at 30 ˚C. In recombinant unactive MAP kinase 2/Erk2, 148 μL of ADBI, 100 μL of magnesium/ATP cocktail, 40 μL of recombinant unactive MAP kinase 2/Erk2 (10 μg), and 2 μL of recombinant MEK1 (0.2 μg) were incubated at 30 ˚C. Time-dependent phosphorylation of recombinant human histone H1.2 catalyzed with protein kinase A was performed in 50 μL of 50 mM Tris-HCl (pH 7.5), 10 mM $MgCl_2$, 0.20 mM ATP, 40 μg of histone H1.2, and 2,500 units of protein kinase A at 37 ˚C. The phosphorylation reactions were stopped by addition of half volume of 3 × SDS-PAGE loading buffer. Zero time samples were prepared using the same component without the enzymes.

Phosphatase assays. Dephosphorylated samples of phosphoproteins were prepared using a 50 mM Tris-HCl buffer (pH 9.0, 0.20 mL) containing 1.0 mM $MgCl_2$, 50 μg protein, and 3.3 units of alkaline phosphatase (incubation at 37 ˚C for 12 h, and then mixing with 0.10 mL of 3 × SDS-PAGE loading buffer). Time-dependent dephosphorylation of bovine milk β-casein were performed in a 50 mM Tris-HCl buffer (pH 9.0, 0.14 mL) containing 1.0 mM $MgCl_2$, 0.7 mg protein, and 165 μunits of alkaline phosphatase at 37 ˚C. Phosphorylated abltide-GST was

prepared as mentioned above, and the solution of the kinase reaction was used in the tyrosine phosphatase assay. Time-dependent dephosphorylation of phosphorylated abltide-GST was performed in 50 mM Tris-HCl buffer (pH 7.0, 0.20 mL) containing 20 μL of phosphorylated Abltide-GST (2 μg) solution, and 0.3 unit of TC-PTP at 30 ˚C. The dephosphorylation reactions were stopped by addition of half volume of 3 × SDS-PAGE loading buffer. Zero time samples were prepared using the same component without the enzymes.

RESULTS

Specific visualization of phosphorylated proteins on a blotting membrane

In order to visualize phosphorylated proteins, we determined the potency of biotin-pendant Zn^{2+}–*Phos-tag* (9) (see Fig. 1) as a phosphate-binding biotin derivative for Western blotting analysis. As the first example, phosphorylated proteins (*i.e.*, α-casein, β-casein, ovalbumin, and pepsin) spotted on a polyvinylidene difluoride (PVDF) membrane were specifically detected at ng levels using an enhanced chemiluminescence (ECL) system and a 4:1 complex of biotin-pendant Zn^{2+}–*Phos-tag* and HRP–SA without a blocking treatment of the membrane. A typical ECL image by dot-blotting analysis is shown in Fig. 2a. No ECL signal was detected on the spots of the corresponding dephosphorylated proteins and the nonphosphorylated proteins (*i.e.*, bovine serum albumin, human serum albumin, carbonic anhydrase, and β-galactosidase). In the absence of the zinc(II) ions (*i.e.*, using a 4:1 complex of biotin-pendant *Phos-tag* ligand and HRP–SA in the presence of 1 mM EDTA), no ECL signals were detected on the spots of phosphorylated proteins (data not shown). Thus, the phosphate-selective ECL signals were produced by the complex of biotin-pendant Zn^{2+}–*Phos-tag* and HRP–SA via the interaction between the zinc(II) ions and the phosphomonoester dianion.

Next, we applied the complex of biotin-pendant Zn^{2+}–*Phos-tag* and HRP–SA to an electroblotting analysis after SDS-PAGE. This application did not require a blocking treatment of a PVDF membrane. The phosphorylation of Abltide-GST incubated with a tyrosine kinase, Abl, and the dephosphorylation of phosphorylated Abltide-GST incubated with a tyrosine phosphatase, TC-PTP, were visualized on PVDF membranes. The Abltide-GST is a recombinant fusion protein of an Abl substrate peptide (Abltide, Glu-Ala-Ilu-*Tyr*-Ala-Ala-Pro-Phe-Ala-Lys-Lys-Lys) tagged by a glutathione *S*-transferase (GST). The $Tyr^{(4)}$ residue of the Abltide section is selectively phosphorylated by Abl. The time courses of the phosphorylation and dephosphorylation are shown in Figs. 2b and 2c, respectively.

Both ECL detections were successively confirmed by a conventional procedure, immunoprobing with the anti-pTyr monoclonal antibody (clone PY20) of the same blots. We also demonstrated similar electroblotting analyses of the phosphorylation of MAP kinase (phosphorylated on the $Thr^{(183)}$ and $Tyr^{(185)}$ residues) incubated with MEK 1 (a Tyr and Ser/Thr dual kinase) and the phosphorylation of histone H1.2 incubated with protein kinase A (a Ser/Thr kinase) (Supplementary Fig. 1). These results indicate that biotin-pendant Zn^{2+}–*Phos-tag* captures various phosphorylated proteins bound on a PVDF membrane.

Visualization of the protein phosphorylation status of A431 cells

We extended the phosphate-specific detection to the analysis of the phosphorylation status of A431 human epidermoid carcinoma cells before and after epidermal growth factor (EGF) stimulation. The EGF-dependent protein phosphorylations in the A431 cell have been well established (13–23); therefore, we selected the cell as the first biological sample. For one-dimensional (1-D) SDS-PAGE (Figs. 3a–g), the molecular weight standards (lane M), the lysate of the cells before (lane 1) or after EGF stimulation (lane 2), and the AP-treated lysate of the cells after EGF stimulation (lane 3) were sequentially applied. Fluorescent gel staining with SYPRO Ruby (Fig. 3a) showed that the total proteins of the lysate applied in each lane were almost equal. Pro-Q Diamond gel staining (Fig. 3b) showed the increase of phosphorylated proteins by EGF stimulation and the decrease of dephosphorylated proteins by AP treatment. Electroblotting analysis using the 4:1 complex of biotin-pendant Zn^{2+}–*Phos-tag* and HRP–SA (Fig. 3c) demonstrated that the ECL signals can represent the phosphorylation status of A431 cells more clearly than the fluorescent gel staining (Fig. 3b). The ECL signals increased by EGF stimulation (lane 2) were greatly diminished by AP treatment of the lysate (lane 3), indicating that the visualized proteins as ECL signals are phosphorylated proteins. The electroblotting analysis also detected a phosphorylated protein, ovalbumin (45 kDa), in the molecular weight standards

(lane M in Fig. 3b). In electroboltting analysis using only HRP–SA, some proteins (*e.g.*, a biotinylated endogenous protein) in the lysate were detected as ECL signals (Fig. 3d). Electroboltting analysis using the 4:1 complex of the biotin-pendant *Phos-tag* ligand and HRP–SA in the presence of 1 mM EDTA (Fig. 3e) shows, however, that the ECL signals (Figs. 3c and d) disappeared completely. These facts suggested that the zinc(II) complexation and the binding of the biotin-pendant to HRP–SA are essential for phosphate-specific detection. The proteins of the cell lysate were also analyzed by immunoblotting using the anti-pTyr antibody (Fig. 3f) and the anti-pSer polyclonal antibody (Fig. 3g). With regard to monitoring the change in the phosphorylation status, the data of the blotting analysis using biotin-pendant Zn^{2+}–*Phos-tag* were compatible with these results obtained with conventional methods using antibodies. In all electroblotting analyses, a nonspecific ECL signal of a marker protein, lysozyme (14 kDa in lane M), was observed using the ECL system (Figs. 3c–g).

Next, we determined the protein phosphorylation status of the EGF-stimulated cells by two-dimensional (2-D) IEF/SDS-PAGE followed by an electroblotting analysis, as shown in Fig. 3h. The ECL signal intensity and number of spots on the membrane remarkably increased in comparison with those before EGF stimulation (see Supplementary Fig. 2). After the ECL detection with biotin-pendant Zn^{2+}–*Phos-tag*, the same membrane was sequentially reprobed with the anti-pTyr antibody and the anti-pSer antibody. Superimposed images of the area surrounded with a dotted square in Fig. 3h were obtained by using biotin-pendant Zn^{2+}–*Phos-tag* (green) and the anti-pTyr antibody (magenta) (Fig. 3i) and biotin-pendant Zn^{2+}–*Phos-tag* (green) and the anti-pSer antibody (magenta) (Fig. 3j). Some proteins detected by both biotin-pendant Zn^{2+}–*Phos-tag* and the antibodies appear as white spots in the superimposed images.

Separation of phosphorylated proteins in a polyacrylamide gel

We synthesized an acrylamide-pendant *Phos-tag* ligand (see Fig. 1 and

experimental procedures) as a novel additive (*i.e.*, a copolymer) of the separating gel for the visualization of phosphorylated proteins by SDS-PAGE. The principle of this detection is the mobility shift of phosphorylated proteins due to reversible phosphate trapping by *Phos-tag* molecules immobilized in the gel. First, we applied a polyacrylamide-bound Zn^{2+}–*Phos-tag* to SDS-PAGE according to the widely accepted Laemmli's method (12). However, the expected phosphate-selective mobility shift was not observed under such general SDS-PAGE conditions (data not shown). Presumably, the alkaline condition (more than pH 9 during the electrophoresis) is beyond the optimum pH (*ca.* 7) for the phosphate trapping of Zn^{2+}–*Phos-tag* (4). Therefore, we investigated the other metal complex acting as a phosphate-trapping molecule at an alkaline pH. The phosphate binding of the *Phos-tag* metal complex at pH 9 was confirmed by MALDI-TOF-MS using phenyl phosphate, phosphoserine, and phosphotyrosine as typical phosphates ($ROPO_3^{2-}$) in the presence of 2 equivalent metal(II) ions (*i.e.*, Mn^{2+}, Cu^{2+}, Co^{2+}, Fe^{2+}, and Ni^{2+}). The acrylamide-pendant *Phos-tag* ligand showed remarkable MS signals of the 1:1 phosphate-binding manganese(II) complexes (*i.e.,* $ROPO_3^{2-}$–[acrylamide-pendant Mn^{2+}–*Phos-tag*]$^{3+}$, see Supplementary Fig. 3). Similar MALDI-TOF-MS signals for corresponding 1:1 phosphate complexes with Zn^{2+}–*Phos-tag* have been reported at a neutral pH (5).

On the basis of the MALDI-TOF-MS results, we conducted SDS-PAGE using polyacrylamide-bound Mn^{2+}–*Phos-tag*. Figure 4 shows the effect of Mn^{2+}–*Phos-tag* on the mobility of phosphorylated proteins (α-casein, β-casein, and ovalbumin) in SDS-PAGE by subsequent Coomassie Brilliant Blue (CBB) staining. In the absence of polyacrylamide-bound Mn^{2+}–*Phos-tag* (*i.e.*, normal SDS-PAGE), the mobilities of α-casein and dephosphorylated α-casein (lane at 0 μM in Fig. 4a), of β-casein and dephosphorylated β-casein (lane at 0 μM in Fig. 4b), and of ovalbumin and dephosphorylated ovalbumin (lane at 0 μM in Fig. 4c) are almost the same. In the presence of polyacrylamide-bound Mn^{2+}–*Phos-tag* (50, 100, and 150 μM), a difference in mobility between the phosphorylated proteins and the corresponding

dephosphorylated proteins (*i.e.*, a mobility shift of the phosphorylated protein against the dephosphorylated protein) is observed. The polyacrylamide-bound *Phos-tag* ligand without Mn^{2+} ions did not show any mobility shifts of phosphorylated proteins (data not shown). The R_f values of all samples become smaller dose-dependently in comparison with those in the absence of Mn^{2+}–*Phos-tag*, which is possibly due to electrostatic interaction between cationic Mn^{2+}–*Phos-tag* and anionic SDS-bound proteins. Interestingly, β-casein appears as 8 bands using 100 μM Mn^{2+}–*Phos-tag* (see Fig. 4b), indicating the existence of at least 8 isotypes with a different number of phosphomonoester dianions.

Simultaneous determination on phosphorylated and dephosphorylated proteins

We quantitatively monitored the enzymatic incorporation or removal of phosphate into proteins using Mn^{2+}–*Phos-tag* SDS-PAGE and CBB staining (see Fig. 5). Normal SDS-PAGE analyses showed that the total protein (the amount of a substrate for kinase or phosphatase) applied at each incubation time was almost equal. In the kinase assays of Abl (Fig. 5a, Abltide–GST as a substrate) and MAP kinase (Fig. 5b, myelin basic protein (MBP) as a substrate) followed by 100 μM Mn^{2+}–*Phos-tag* SDS-PAGE and CBB staining, the slower (higher) migration bands increased time-dependently, while the faster (lower) migration bands decreased. Successive immunoblotting analyses using the anti-pTyr antibody (Fig. 5a) and the anti-pMBP antibody (recognized phosphorylated $Thr^{(97)}$ residue) (Fig. 5b) showed that the slower migration bands are phosphorylated proteins. Treatment of the Mn^{2+}–*Phos-tag* SDS-PAGE gel with EDTA before the immunoblotting analyses is necessary for efficient transfer of the phosphorylated proteins to a PVDF membrane without trapping by the *Phos-tag* molecule (see Methods). In the phosphatase assays of AP (Fig. 5c, β-casein as a substrate) and TC-PTP (Fig. 5d, phosphorylated Abltide–GST as a substrate) followed by Mn^{2+}–*Phos-tag* SDS-PAGE and CBB staining, the slower (higher) migration bands decreased

time-dependently, while the faster (lower) migration bands increased. These results indicate that acrylamide-pendant Mn^{2+}–*Phos-tag* preferentially captures phosphomonoester dianions bound to Ser, Thr, and Tyr residues as well as biotin-pendant Zn^{2+}–*Phos-tag*. Thus, Mn^{2+}–*Phos-tag* SDS-PAGE has enabled the simultaneous determination of phosphorylated and corresponding dephosphorylated proteins in a polyacrylamide gel.

DISCUSSION

In this paper, we have described two methods using *Phos-tag* molecules for the visualization of protein phosphorylation and dephosphorylation. The methods are independent on the amino acid residues; thus, protein phosphorylation can be comprehensively detected. One method is the application of biotin-pendant Zn^{2+}–*Phos-tag* and HRP–SA to Western blotting analysis: protein samples are first separated by electrophoresis and then electroblotted to a PVDF membrane and detected as ECL signals. We succeeded in the sensitive and specific detection of phosphorylated proteins on serine, threonine, and tyrosine residues using the ECL system. The blot-staining method has a general advantage over gel-staining methods with regard to the long-term storage of protein-blotted membranes. The other method is the application of polyacrylamide-bound Mn^{2+}–*Phos-tag* to SDS-PAGE for the separation of phosphorylated proteins in the gel. By means of the subsequent general method of CBB staining, phosphorylated proteins can be visualized as a slower migration band compared with a corresponding dephosphorylated protein. This quantitative method revealed the existence of the isotypes of a multi-phosphorylated protein (*e.g.*, β-casein) as different migration bands. Additionally, it is appropriate for the screening of an activator or an inhibitor of protein kinase and phosphatase.

The biotin-pendant Zn^{2+}–*Phos-tag* was reported as a novel probe of multi-phosphopeptides to detect the on-chip phosphorylations by the SPR imaging technique (9). Previously, another SPR detection system with the anti-pTyr antibody was proposed (24). Antibodies whose epitopes are pSer, pThr, or pTyr are commercially available and can be applied to phosphorylation detection on the SPR. However, multiple antibodies are required for the peptide array, on which many kinase substrates are immobilized. Therefore, the *Phos-tag* molecule, which is not dependent on the amino acid residue, was very useful in a system with an array format. In a similar fashion, it is worthwhile to consider using the biotin-pendant Zn^{2+}–*Phos-tag* in Western blotting analysis for evaluating whole phosphorylated

proteins from the cell lysate on a PVDF membrane. In addition, the application can increase the chances of finding a new phosphorylated protein. Classical detection of phosphorylated proteins usually requires the use of autoradiography after the incorporation of isotopic [^{32}P]orthophosphate into cultured cells or subcellular fractions by protein kinases (14–21). However, this approach is limited to specimens amenable to radiolabeling and poses certain safety and disposal problems. Furthermore, phosphorylated proteins on a PVDF membrane can be detected by immunoblotting analysis using antibodies against phosphorylated amino acid residues (25–27). Unfortunately, the specificity of antibodies depends on the quality of the antibody, and the antibodies are often sensitive to the amino acid sequence context. Although a few high-quality clones of antibodies to phosphorylated tyrosine are commercially available, the binding specificities of some anti-pSer and anti-pThr antibodies are dependent on the microenvironmental structures of phosphorylated residues in the proteins. Compared with these traditional approaches, our established method offers significant advantages: (i) The radioactivity is avoided; (ii) The blocking treatment of a PVDF membrane is not necessary; and (iii) The binding specificity of the *Phos-tag* molecule is independent on the amino acid sequence context. Furthermore, the *Phos-tag* method can be fully followed by downstream procedures, such as antibody reprobing, mass spectrometry, or Edman sequencing.

The Mn^{2+}–*Phos-tag* was utilized as a novel phosphate-affinity SDS-PAGE. The polyacrylamide-bound Mn^{2+}–*Phos-tag* showed preferential trapping of the phosphorylated proteins without disordering (waving or tailing of protein bands) of the migration image. The 1:1 phosphate-bound Mn^{2+}–*Phos-tag* complexes were confirmed by MALDI-TOF-MS at an alkaline pH for the general SDS-PAGE. A relevant X-ray crystal structure of the dimanganese complex with the *Phos-tag* ligand (alkoxide form) was reported as an acetate-bridging species (28). Our established method requires a general mini-slab PAGE system and an additive, acrylamide-pendant Mn^{2+}–*Phos-tag* without any special apparatuses, radioisotopes,

or fluorescent probes. The Mn^{2+}–*Phos-tag* SDS-PAGE can identify the time-course ratio of phosphorylated and dephosphorylated proteins in an SDS-PAGE gel.

The phosphorylation status of a particular protein is determined by the equilibrium of the opposing activities of protein kinase and phosphatase. Perturbations in the equilibrium fundamentally affect the numbers of cellular events and are also involved in many diseases. Therefore, the development of a more specific and efficient method to detect protein phosphorylation has attracted great interest toward phosphoproteome studies in the biological and medical fields. We believe that phosphoproteomics would progress greatly by combining our *Phos-tag* technology and existing methods using high-quality antibodies (27) and convenient mass spectrometers (29–31).

ACKNOWLEDGEMENTS

This work was supported by Grants-in-Aid for Scientific Research (B) (15390013) and for Young Scientists (B) (17790034) from the Ministry of Education, Culture, Sports, Science, and Technology of Japan and by a research grant from Hiroshima University Fujii Foundation.

References

1. Hunter T. (1995) Protein kinases and phosphatases: the yin and yang of protein phosphorylation and singnaling. *Cell* **80**, 225–236
2. Hunter T. (2000) Signaling–2000 and beyond. *Cell* **100**, 113–127
3. Commercially available at http://www.phos-tag.com.
4. Kinoshita, E., Takahashi, M., Takeda, H., Shiro, M., and Koike T. (2004) Recognition of phosphate monoester dianion by an alkoxide-bridged dinuclear zinc(II) complex. *Dalton Trans.* 1189–1193
5. Takeda, H., Kawasaki, A., Takahashi, M., Yamada, A., and Koike, T. (2003) Matrix-assisted laser desorption/ionization time-of-flight mass spectrometry of phosphorylated compounds using a novel phosphate capture molecule. *Rapid Commun. Mass Spectrom.* **17**, 2075–2081
6. Hirano, K., Matsui, H., Tanaka, T., Matsuura, F., Satouchi, K., and Koike, T. (2004) Production of 1,2-didocosahexaenoyl phosphatidylcholine by bonito muscle lysophosphatidylcholine/transacylase. *J. Biochem*. **136**, 477–483

7 Tanaka, T., Tsutsui, H., Hirano, K., Koike, T., Tokumura, A., and Satouchi, K. (2004) Quantitative analysis of lysophosphatidic acid by time-of-flight mass spectrometry using a phosphate-capture molecule. *J. Lipid Res.* **45**, 2145–2150

8. Kinoshita, E., Yamada, A., Takeda, H., Kinoshita-Kikuta, E., and Koike, T. (2005) Novel immobilized zinc(II) affinity chromatography for phosphopeptides and phosphorylated proteins. *J. Sep. Sci.* **28**, 155–162
9. Inamori, K. Kyo, M., Nishiya, Y., Inoue, Y., Sonoda, T., Kinoshita, E., Koike, T., and Katayama, Y. (2005) Detection and quantification of on-chip phosphorylated peptides by surface plasmon resonance imaging techniques using a phosphate capture molecule. *Anal. Chem.* **77**, 3979–3985
10. Steinberg, T. H., Agnew, B. J., Gee, K. R., Leung, W. Y., Goodman, T., Schulenberg, B., Hendrickson, J., Beechem, J. M., Haugland, R. P., and Patton, W. F. (2003) Global quantitative phosphoprotein analysis using multiplexed

proteomics technology. *Proteomics* **3**,1128-1144

11. Berggren, K., Chernokalskaya, E., Steinberg, T. H., Kemper, C., Lopez, M. F., Diwu, Z., Haugland, R. P., and Patton, W. F. (2000) Background-free, high sensitivity staining of proteins in one- and two-dimensional sodium dodecyl sulfate-polyacrylamide gels using a luminescent ruthenium complex. *Electrophoresis* **21**, 2509–2521
12. Laemmli, U. K. (1970) Cleavage of structural proteins during the assembly of the head of bacteriophage T4. *Nature* **227**, 680–685
13. Carpenter, G., and Cohen, S. (1979) Epidermal growth factor. *Annu. Rev. Biochem.* **48**,193-216
14. Carpenter, G., King, L., Jr., and Cohen, S. (1979) Rapid enhancement of protein phosphorylation in A-431 cell membrane preparations by epidermal growth factor. *J. Biol. Chem.* **254**, 4884–4891
15. Cohen, S., Carpenter, G., and King, L., Jr. (1980) Epidermal growth factor-receptor-protein kinase interactions. Co-purification of receptor and epidermal growth factor-enhanced phosphorylation activity. *J. Biol. Chem.* **255**, 4834–4842
16. Linsley, P. S., and Fox, C. F. (1980) Controlled proteolysis of EGF receptors: evidence for transmembrane distribution of the EGF binding and phosphate acceptor sites. *J. Suparmol. Struct.* **14**, 461–471
17. Hunter, T., and Cooper, J. A. (1981) Epidermal growth factor induces rapid tyrosine phosphorylation of proteins in A431 human tumor cells. *Cell* **24**, 741–752
18. Cooper, J. A., and Hunter, T. (1981) Similarities and differences between the effects of epidermal growth factor and Rous sarcoma virus. *J. Cell Biol.* **91**, 878–883
19. Ghosh-Dastidar, P., and Fox, C. F. (1983) Epidermal growth factor and epidermal growth factor receptor-dependent phosphorylation of a M_r = 34,000 protein substrate for $pp60^{src}$. *J. Biol. Chem.* **258**, 2041–2044

20. Meisenhelder, J., Suh, P. G., Rhee, S. G., and Hunter, T. (1989) Phospholipase C-γ is a substrate for the PDGF and EGF receptor protein-tyrosine kinases in vivo and in vitro. *Cell* **57**, 1109–1122
21. Li, S., Couvillon, A. D., Brasher, B. B., and Van Etten, R. A. (2001) Tyrosine phosphorylation of Grb2 by Bcr/Abl and epidermal growth factor receptor: a novel regulatory mechanism for tyrosine kinase signaling. *EMBO J.* **20**, 6793–6804
22. Lim, Y. P., Diong, L. S., Qi, R., Druker, B. J., and Epstein, R. J. (2003) Phosphoproteomic fingerprinting of epidermal growth factor signaling and anticancer drug action in human tumor cells. *Mol. Cancer. Ther.* **2**, 1369-1377
23. Chelius, D., Zhang, T., Wang, G., and Shen, R. F. (2003) Global protein identification and quantification technology using two-dimensional liquid chromatography nanospray mass spectrometry. *Anal. Chem.* **75**, 6658-6665
24. Houseman, B. T., Huh, J. H., Kron, S. J., and Mrksich, M. (2002) Peptide chips for the quantitative evaluation of protein kinase activity. *Nat. Biotechnol.* **20**, 270–274
25. Czernik A. J., Girault, J. A., Nairn, A. C., Chen, J., Snyder, G., Kebabian, J., and Greengard, P. (1991) Production of phosphorylation state-specific antibodies. *Methods Enzymol.* **201**, 264–283
26. Epstein, R. J., Druker, B. J., Roberts, T. M., and Stiles, C. D. (1992) Synthetic phosphopeptide immunogens yield activation-specific antibodies to the c-erbB-2 receptor. *Proc. Natl. Acad. Sci. USA* **89**, 10435–10439
27. Kaufmann, H., Bailey, J. E., and Fussenegger, M. (2001) Use of antibodies for detection of phosphorylated proteins separated by two-dimensional gel electrophoresis. *Proteomics* **1**, 194–199
28. Suzuki, M., Sugisawa, T., Senda, H., Oshio, H., and Uehara, A. (1989) Synthesis and characterization of a novel tetranuclear manganese(II,III,III,II) mixed valence complex. *Chem. Lett.* 1091–1094
29. Sloane, A. J., Duff, J. L., Wilson, N. L., Gandhi, P. S. Hill, C. J., Hopwood, F. G.

Smith, P. E., Thomas, M. L., Cole, R. A., Packer, N. H., Breen, E. J., Cooley, P. W., Wallace, D. B., Williams, K. L., and Gooley A. A. (2002) High throughput peptide mass fingerprinting and protein macroarray analysis using chemical printing strategies. *Mol. Cell Proteomics* **1**, 490–499

30. Nakanishi, T., Ohtsu, I., Furuta, M., Ando, E., and Nishimura, O. (2005) Direct MS/MS analysis of proteins blotted on membranes by a matrix-assisted laser desorption/ionization-quadrupole ion trap-time-of-flight tandem mass spectrometer. *J. Proteome Res.* **4**, 743–747

31 Ohtsu, I., Nakanishi, T., Furuta, M., Ando, E., and Nishimura, O. (2005) Direct matrix-assisted laser desorption/ionization time-of-flight mass spectrometric identification of proteins on membrane detected by western blotting and lectin blotting. *J. Proteome Res.* **4**, 1391–1396

FIGURE LEGENDS

FIG. 1. **Structures of biotin-pendant and acrylamide-pendant *Phos-tag* ligands and scheme of the reversible capturing of a phosphomonoester dianion (*R*OPO$_3^{2-}$) by Zn^{2+}–*Phos-tag* and Mn^{2+}–*Phos-tag*.**

FIG. 2 **Chemiluminescence detection of phosphorylated proteins on PVDF membranes using biotin-pendant Zn^{2+}–*Phos-tag* and HRP–SA.** (a) Dot-blotting analysis of four nonphosphorylated proteins (bovine serum albumin, human serum albumin, carbonic anhydrase, and β-galactosidase), four phosphorylated proteins (α-casein, β-casein, ovalbumin, and pepsin), and the corresponding dephosphorylated proteins (AP-treated). (b) Electroblotting analysis of the phosphorylation of Abltide-GST (0.13 μg protein/lane) incubated with a tyrosine kinase, Abl. (c) Electroblotting analysis of the dephosphorylation of phosphorylated Abltide-GST (50 ng proteins/lane) incubated with a tyrosine phosphatase, TC-PTP. After elimination of biotin-pendant Zn^{2+}–*Phos-tag* and HRP–SA from the membranes (b and c), the remaining phosphorylated Abltide-GST was probed using the HRP–anti-pTyr antibody. The incubation time is shown above each lane.

FIG. 3 **Comparison of different detection methods for 1-D SDS-PAGE (a – g) and 2-D IEF/SDS-PAGE (h – j) of A431 cell lysate.** (a) Fluorescent gel staining with SYPRO Ruby (*i.e.*, staining of all proteins). (b) Fluorescent gel staining with Pro-Q Diamond (*i.e.*, staining of the phosphorylated protein). (c) Electroblotting analysis (chemiluminescence detection) using biotin-pendant Zn^{2+}–*Phos-tag* and HRP–SA. (d) Electroblotting analysis (chemiluminescence detection) using HRP–SA. (e) Electroblotting analysis (chemiluminescence detection) using the HRP–SA complex with the biotin-pendant *Phos-tag* ligand in the presence of 1 mM EDTA. (f) Electroblotting analysis (chemiluminescence detection) using the HRP–anti-pTyr antibody. (g) Electroblotting analysis (chemiluminescence

detection) using the anti-pSer antibody and the HRP–anti-IgG antibody. Each lane (a – g) contains 7.5 *μ*g protein of the A431 cell lysate before (lane 1) or after (lane 2) EGF stimulation or 7.5 *μ*g protein of the AP-treated lysate of EGF-stimulated A431 cells (lane 3). The molecular weight standards (MW: 205, 116, 97, 80, 66, 55, 45 (ovalbumin), 30, 21, and 14 (lysozyme) kDa from the top) are shown in lane M. (h) Electroblotting 2-D analysis (chemiluminescence detection) of the EGF-stimulated A431 cell lysate (50 *μ*g proteins) using biotin-pendant Zn^{2+}–*Phos-tag* and HRP–SA. The blot was successively probed with the HRP–anti-pTyr antibody and the anti-pSer antibody/HRP–anti-IgG antibody. Superimposed images of the area surrounded with a dotted square in h: (i) using biotin-pendant Zn^{2+}–*Phos-tag* (green) and the anti-pTyr antibody (magenta); (j) using biotin-pendant Zn^{2+}–*Phos-tag* (green) and the anti-pSer antibody (magenta). Proteins detected by both methods appear as white spots in i and j.

FIG. 4 **SDS-PAGE of phosphorylated proteins and the corresponding dephosphorylated proteins in the absence and presence of polyacrylamide-bound Mn^{2+}–*Phos-tag* (50, 100, and 150 *μ*M).** (a) α-casein with 10% polyacrylamide gel, (b) β-casein with 10% polyacrylamide gel, and (c) ovalbumin with 7.5% polyacrylamide gel. The phosphorylated and dephosphorylated proteins (0.30 *μ*g protein/lane) were applied in the left and right lanes, respectively, for each run of electrophoresis. The R_f value of 1.0 is defined as the position of bromophenol blue dye. All SDS-PAGE gels were stained with CBB dye.

FIG. 5 **Kinase and phosphatase assays by Mn^{2+}–*Phos-tag* SDS-PAGE (10 – 12.5% polyacrylamide containing 100 *μ*M polyacrylamide-bound Mn^{2+}–*Phos-tag*).** (a) Phosphorylation of Abltide-GST (0.10 *μ*g protein/lane) incubated with Abl in 12.5% polyacrylamide gel. After Mn^{2+}–*Phos-tag* SDS-PAGE, immunoblotting analysis (chemiluminescence detection) was conducted using the

HRP–anti-pTyr antibody. (b) Phosphorylation of MBP (0.56 μg protein/lane) incubated with MAP kinase in 12.5% polyacrylamide gel. After Mn^{2+}–*Phos-tag* SDS-PAGE, immunoblotting analysis (chemiluminescence detection) was conducted using the anti-pMBP antibody/HRP–anti-IgG antibody. (c) Dephosphorylation of β-casein (0.30 μg protein/lane) incubated with AP in 10% polyacrylamide gel. (d) Dephosphorylation of phosophorylated Abltide-GST (0.10 μg protein/lane) incubated with a tyrosine phosphatase, TC-PTP in 12.5% polyacrylamide gel. The incubation time is shown above each lane. Normal SDS-PAGE and Mn^{2+}–*Phos-tag* SDS-PAGE gels were stained with CBB dye.

Fig. 1

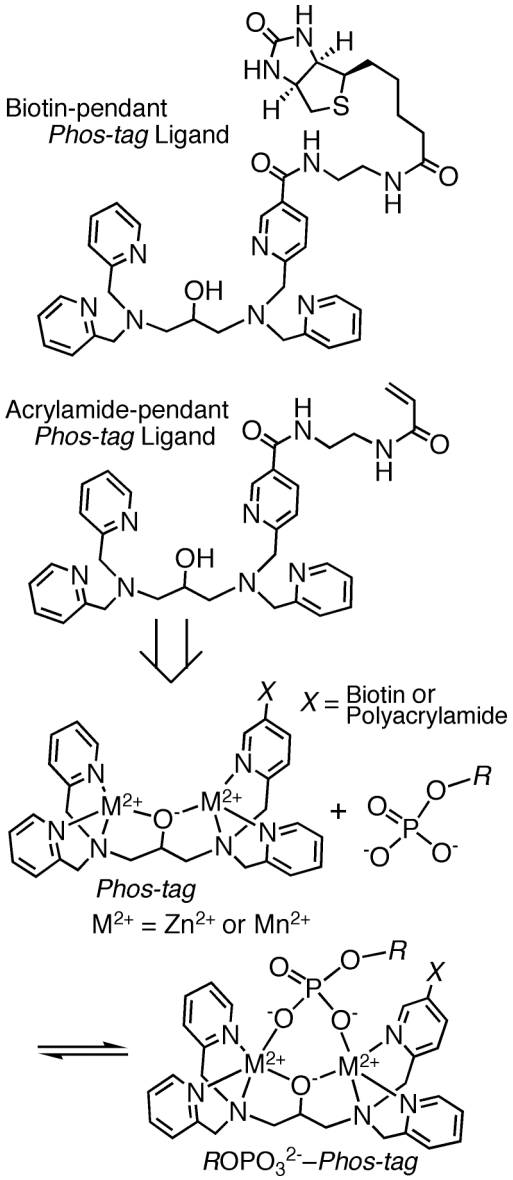
Biotin-pendant
Phos-tag Ligand
Acrylamide-pendant
Phos-tag Ligand
X = Biotin or
Polyacrylamide
Phos-tag
M2+ = Zn2+ or Mn2+
ROPO32−–Phos-tag

Fig. 2

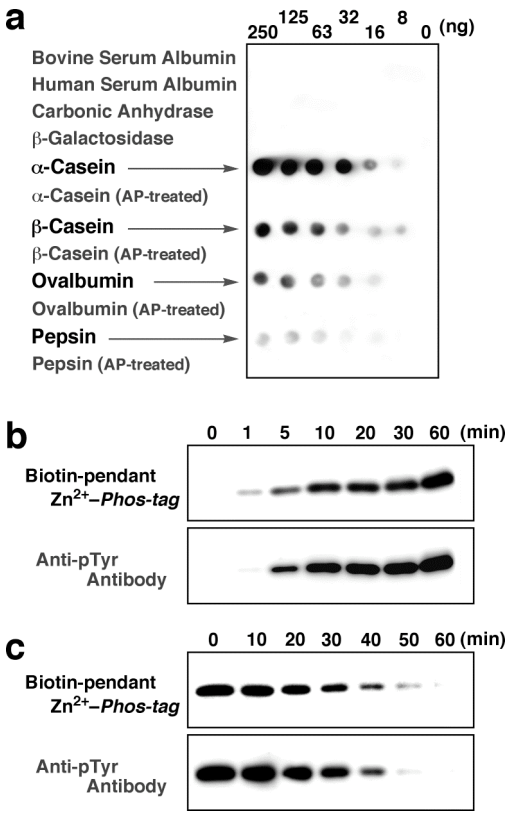
a
250 125 63 32 16 8 0 (ng)
Bovine Serum Albumin
Human Serum Albumin
Carbonic Anhydrase
β-Galactosidase
α-Casein
α-Casein (AP-treated)
β-Casein
β-Casein (AP-treated)
Ovalbumin
Ovalbumin (AP-treated)
Pepsin
Pepsin (AP-treated)
b
0 1 5 10 20 30 60 (min)
Biotin-pendant
Zn2+–Phos-tag
Anti-pTyr
Antibody
c
0 10 20 30 40 50 60 (min)
Biotin-pendant
Zn2+–Phos-tag
Anti-pTyr
Antibody

Fig. 3

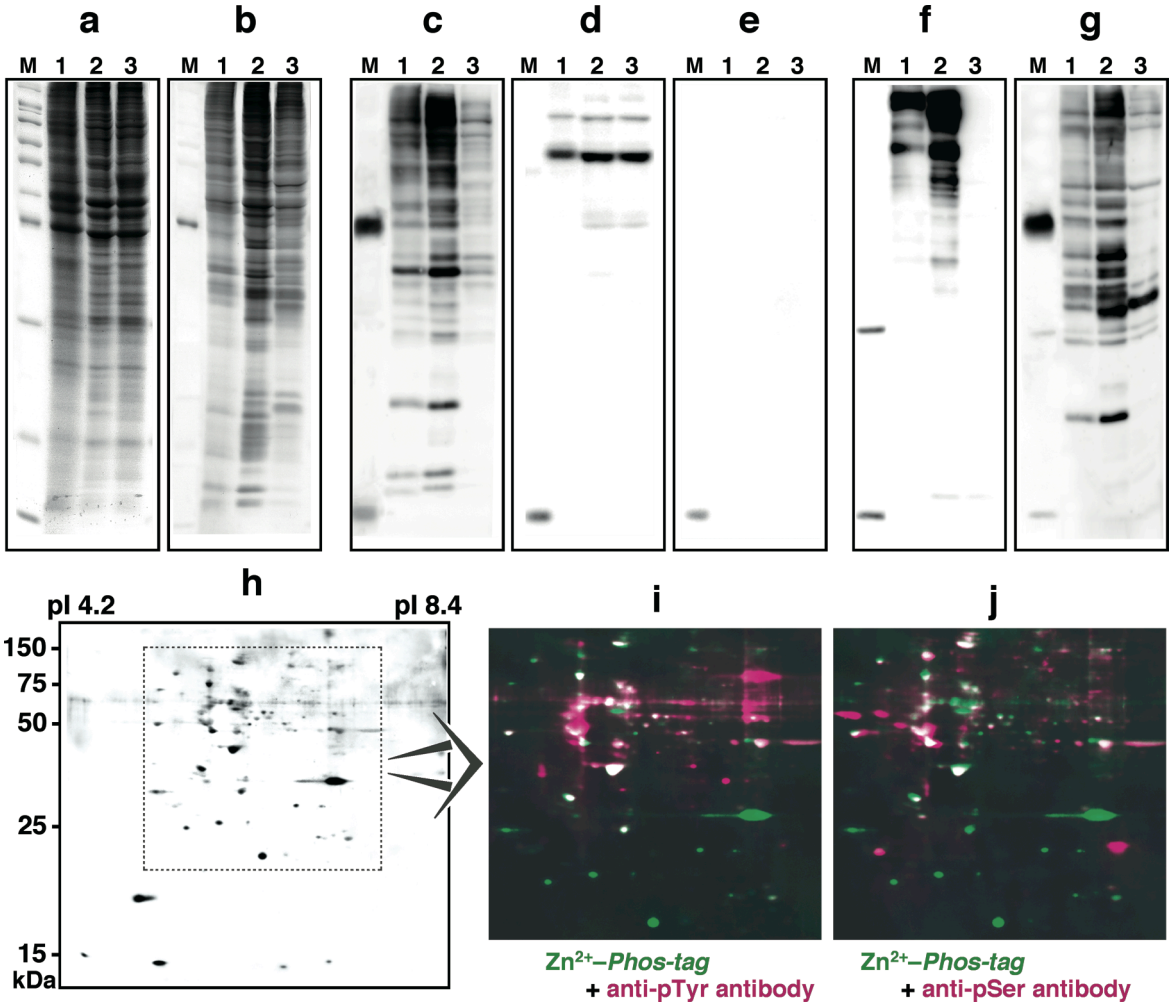
a
b
c
d
e
f
g
M 1 2 3
h
pI 4.2
pI 8.4
150
75
50
25
15
kDa
i
j
Zn2+–Phos-tag
+ anti-pTyr antibody
Zn2+–Phos-tag
+ anti-pSer antibody

Fig. 4

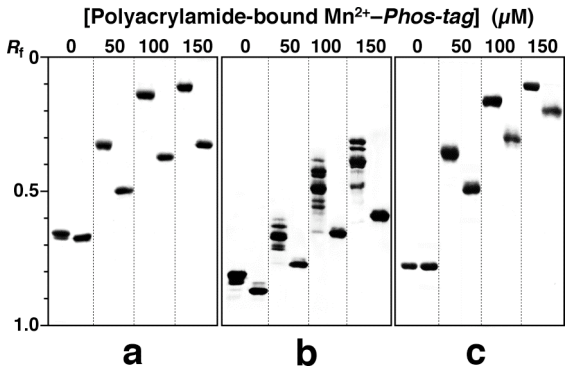
[Polyacrylamide-bound Mn2+–Phos-tag] (μM)
Rf
0
50
100
150
0
50
100
150
0
50
100
150
0
0.5
1.0
a
b
c

Fig. 5

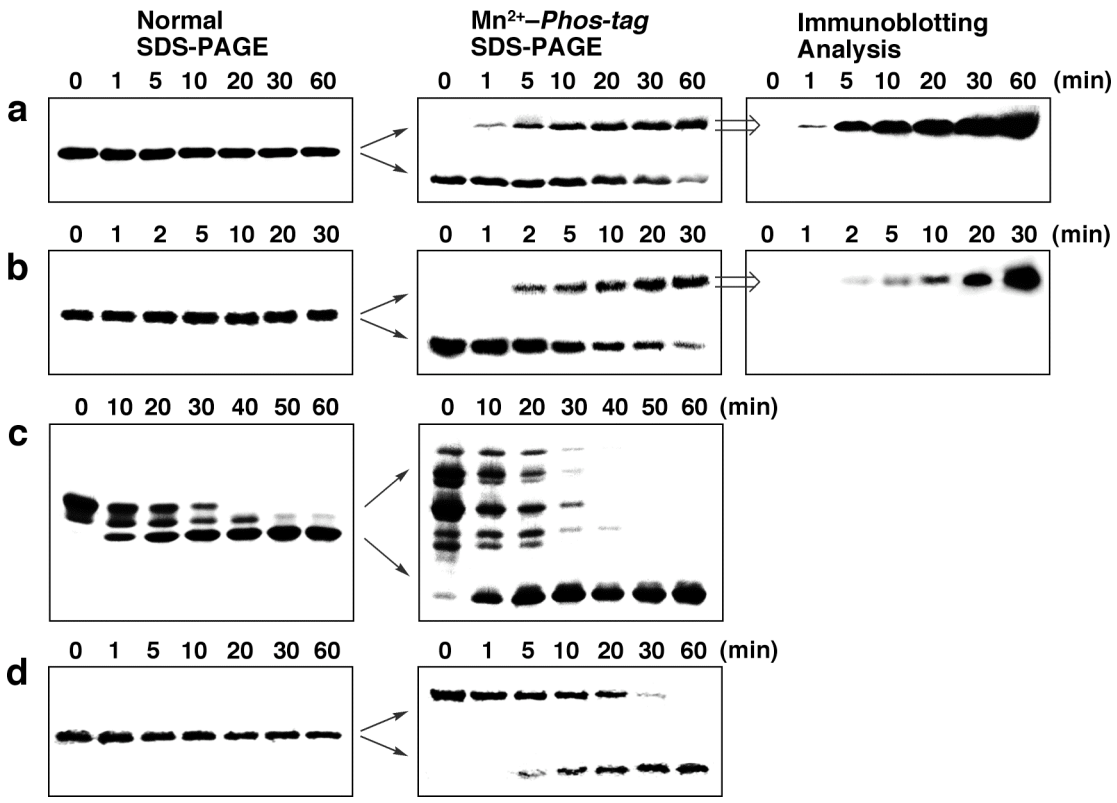
Normal
SDS-PAGE
Mn2+–Phos-tag
SDS-PAGE
Immunoblotting
Analysis
a
0 1 5 10 20 30 60
0 1 5 10 20 30 60
0 1 5 10 20 30 60 (min)
b
0 1 2 5 10 20 30
0 1 2 5 10 20 30
0 1 2 5 10 20 30 (min)
c
0 10 20 30 40 50 60
0 10 20 30 40 50 60 (min)
d
0 1 5 10 20 30 60
0 1 5 10 20 30 60 (min)

SUPPLEMENTARY FIGURE 1

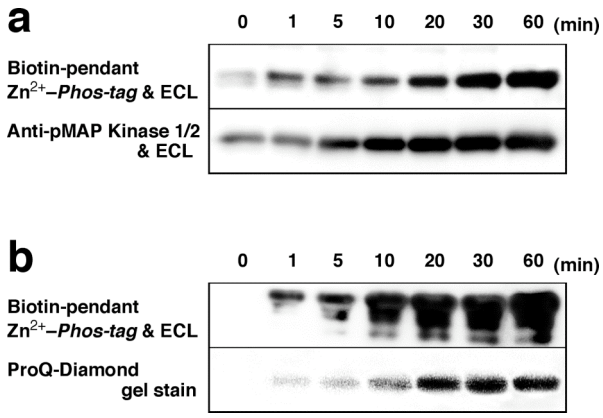

FIG. S1. Chemiluminescence detection of other protein phosphorylations using biotin-pendant Zn^{2+}–*Phos-tag* and HRP–SA. (**a**) Electroblotting analysis of phosphorylation of unactive MAP kinase-GST (0.20 μg protein/lane) incubated with a Tyr and Ser/Thr dual kinase, MEK 1. The unactive MAP kinase-GST is a recombinant fusion protein of a nonphosphorylated MAP kinase 2 tagged by a GST, and the MAP kinase 2 is phosphorylated at $Thr^{(183)}$ and $Tyr^{(185)}$ residues by MEK1. After the chemiluminescence detection of phosphorylated MAP kinase-GST with biotin-pendant Zn^{2+}–*Phos-tag*, the same blot was reprobed with the anti-pMAP kinase 1/2 monoclonal antibody (clone 12D4), which recognizes the dual phosphorylations. (**b**) Electroblotting analysis of phosphorylation of recombinant human histone H1.2 (1 μg protein/lane) incubated with a Ser/Thr kinase, protein kinase A. Phosphorylation of histone H1.2 was also confirmed by Pro-Q Diamond gel staining. The incubation time is shown above each lane.

SUPPLEMENTARY FIGURE 2

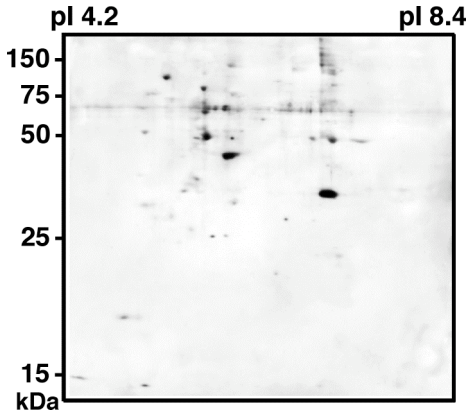

FIG. S2. Chemiluminescence detection of EGF-unstimulated A431 cell lysate (50 *μ*g proteins) using biotin-pendant Zn^{2+}–*Phos-tag* and HRP–SA after 2-D IEF/SDS-PAGE analysis. The ECL signal intensity and number of spots on PVDF membrane are less than those of EGF-stimulated A431 cell lysate (50 *μ*g proteins, see Fig. 3h).

SUPPLEMENTARY FIGURE 3

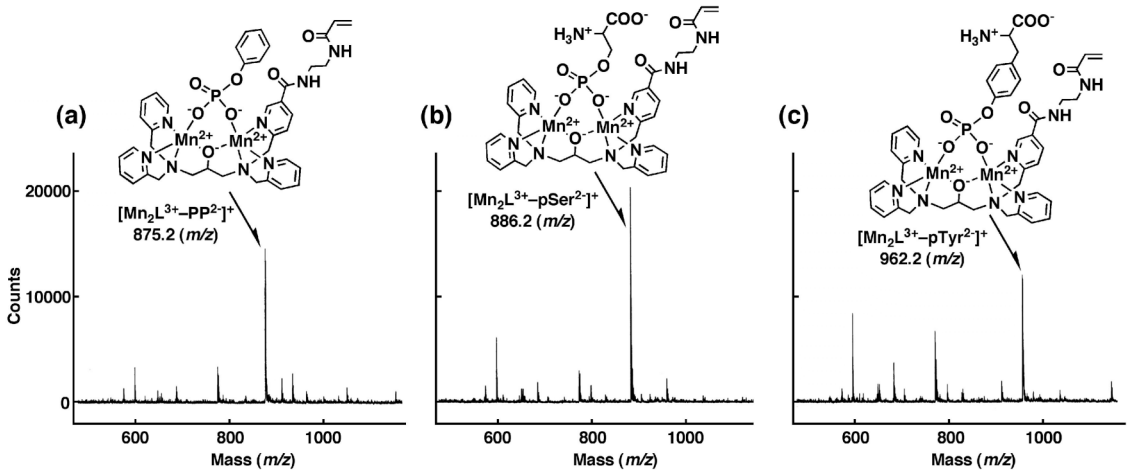

FIG. S3. MALDI-TOF mass spectra (positive mode) for 1:1 complexes of phosphorylated compounds and acrylamide-pendant Mn^{2+}–*Phos-tag*. Each sample (0.20 nmol phosphate) was dissolved in a mixed solution of Harmane (a matrix molecule, 5 ng) in aceton (0.5 μL) and a 10 mM borate-NaOH buffer (pH 9.0, 0.5 μL) containing acrylamide-pendant *Phos-tag* ligand (L, 0.20 nmol) and $MnCl_2$ (0.40 nmol): (a) Phenyl phosphate (PP^{2-}). (b) Phosphorylated serine ($pSer^{2-}$). (c) Phosphorylated tyrosine ($pTyr^{2-}$).